Neuroscience Research xxx (xxxx) xxx

Contents lists available at ScienceDirect

Neuroscience Research

journal homepage: www.sciencedirect.com/journal/neuroscience-research

Coexistence of sensory qualities and value representations in human orbitofrontal cortex

Takaaki Yoshimoto [a], Shuntaro Okazaki [a], Motofumi Sumiya [k,l], Haruka K. Takahashi [c], Eri Nakagawa [a], Takahiko Koike [a,b], Ryo Kitada [m], Shiki Okamoto [d], Masanori Nakata [e], Toshihiko Yada [f,g], Hirotaka Kosaka [h], Norihiro Sadato [a,b,*], Junichi Chikazoe [b,i,j,*]

[a] Division of Cerebral Integration, National Institute for Physiological Sciences, Okazaki 444-8585, Japan
[b] Department of Physiological Sciences, SOKENDAI (The Graduate University for Advanced Studies), Hayama 240-0193, Japan
[c] Kao Corporation, Odawara 250-0002, Japan
[d] Second Department of Internal Medicine (Endocrinology, Diabetes and Metabolism, Hematology, Rheumatology), Graduate School of Medicine, University of the Ryukyus, Okinawa 903–0215, Japan
[e] Department of Physiology, Faculty of Medicine, Wakayama Medical University School of Medicine, Wakayama 641-8509, Japan
[f] Division of Integrative Physiology, Kansai Electric Power Medical Research Institute, Kobe 650-0047, Japan
[g] Diabetes, Metabolism and Endocrinology, Kobe University Graduate School of Medicine, Kobe 650-0017, Japan
[h] Department of Neuropsychiatry, University of Fukui, Fukui 910-1193, Japan
[i] Section of Brain Function Information, Supportive Center for Brain Research, National Institute for Physiological Sciences, Okazaki 444-8585, Japan
[j] ARAYA Inc., Tokyo 107-6024, Japan
[k] Japan Society for the Promotion of Science, Tokyo, 102-0083, Japan
[l] Graduate School of the Humanities, Senshu University, Tokyo, 101-8425, Japan
[m] Graduate School of Intercultural Studies, Kobe University, Kobe, 657-8501, Japan

ARTICLE INFO

Keywords:
Functional MRI
Gustatory experience
Human
Multivoxel pattern analysis
Reward

ABSTRACT

Despite the multiple regions and neural networks associated with value-based decision-making, the orbitofrontal cortex (OFC) is possible a particularly important one. Although the role of the OFC in reinforcer devaluation tasks, which assess the ability to represent identity, sensory qualities, and subjective values of the expected outcomes, has been established, the specific aspect represented in this area remains unclear. In this study, using functional magnetic resonance imaging, wherein participants rated the palatability of 128 food items using photographs, we investigated whether the human OFC represents object identity, sensory qualities, or value. Employing many items helped us dissociate object identity from sensory qualities and values; the inferred sensory qualities of identical items were manipulated by a change in metabolic state. Moreover, value differences between items were analytically controlled by employing a technique similar to age adjustment. The palatability ratings for food items significantly decreased after a meal. Using representational similarity analysis, we confirmed that the OFC represents value. Moreover, identical items were represented similarly in the lateral OFC in a given metabolic state; however, these representations were altered post-feeding. Importantly, this change was not explained by subjective value, suggesting that the OFC represents sensory quality and value, but not object identity.

1. Introduction

Decision making is a cognitive process in which multidimensional information must be integrated. For example, when we decide what to eat at a restaurant, we infer gustatory experience from the photos and descriptions on the menu while considering our current metabolic state (i.e., satiated or hungry). Even if the dessert options themselves are identical, inferred gustatory experiences are not the same at the time of the first course as when dessert is ordered, suggesting that the inferred sensory qualities and identity can be dissociated under certain conditions. As in the old proverb, “hunger is the best sauce,” the sensory qualities of food are dynamically altered by changes in one’s internal

* Corresponding authors at: Department of Physiological Sciences, SOKENDAI (The Graduate University for Advanced Studies), Hayama 240-0193, Japan.
E-mail addresses: sadato@nips.ac.jp (N. Sadato), chikazoe@nips.ac.jp (J. Chikazoe).

https://doi.org/10.1016/j.neures.2022.02.004
Received 9 December 2021; Received in revised form 7 February 2022; Accepted 20 February 2022
Available online 23 February 2022

metabolic state while the food identity is stably represented. By integrating such information, an individual estimates the value of each option in deciding what to eat. Although multiple regions and neural networks have been associated with hedonic and metabolic processes governing food choices (Hare et al., 2009; Janssen et al., 2017; van der Laan et al., 2014; Voigt et al., 2020, 2021), we focused on the orbitofrontal cortex (OFC) because this region integrates sensory and visceral information, providing a potential biological basis for such decision-making (Kringelbach, 2005). Specifically, a growing body of research has shown that the OFC encodes the predicted outcomes that follow either sensory events or behavioral choices (Rudebeck et al., 2013; Schoenbaum et al., 2009). In particular, studies on rodents, monkeys, and humans have consistently demonstrated that the OFC plays a critical role in reinforcer devaluation, in which specific food rewards are provided until satiated or paired with illness (Gallagher et al., 1999; Gremel and Costa, 2013; Izquierdo, 2004; Pickens et al., 2005; Reber et al., 2017; Rudebeck et al., 2013; West et al., 2013). Such procedures, which decrease the reinforcer value (i.e., the reward), are commonly termed "reinforcer devaluation" (Stalnaker et al., 2015; Schoenbaum et al., 2009). While healthy participants prefer an option that leads to the food with which they are not sated, OFC-lesioned animals or patients show no such preference (Gallagher et al., 1999; Reber et al., 2017; Rudebeck et al., 2013).

However, the specific function of this region remains under debate (Rudebeck and Murray, 2014; Schoenbaum et al., 2011; Stalnaker et al., 2015), partially because of the complexity of the reinforcer devaluation task. Although behavior is driven by composite representations of identity, sensory qualities, and subjective values of expected outcomes in this paradigm (Howard et al., 2015; Rudebeck and Murray, 2014), the emphasized aspect of the task varies across studies. Although several studies have focused on the involvement of the OFC in value representations (Gallagher et al., 1999; Kringelbach et al., 2003; Rudebeck et al., 2013), others have emphasized representations of the sensory qualities or food identity (Burke et al., 2008; Gremel and Costa, 2013; Schoenbaum et al., 2011). Indeed, there are several difficulties in dissociating these representations in the reinforcer devaluation task. For example, because different taste rewards evoke different sensory qualities, differences in identity and sensory qualities cannot be dissociated should the reward type given be small, as in animal experiments. Moreover, devaluation alters the sensory qualities of expected outcomes, as well as their subjective value (Rudebeck and Murray, 2014), although their identity remains the same (e.g., orange juice can be identified as orange juice even if it does not taste good after devaluation). Thus, it remains unclear whether the OFC represents identity, sensory quality, or the subjective value of the expected outcome.

In this study, we sought to answer this question using a non-selective devaluation paradigm with many reward types. In our functional magnetic resonance imaging (fMRI) experiment, participants rated the palatability of 128 various food photos before and after meals on two experimental days. By employing representational similarity analysis (Kriegeskorte, 2008), we investigated where in the brain the representations of identical objects were maintained through pairs of the same or different metabolic states. If the OFC represents object identity, the representations of identical objects would be invariant across different metabolic states, whereas if the OFC represents the inferred sensory qualities but not identity, those representations would be maintained only in the same metabolic state. Furthermore, we investigated whether such representations could be explained by differences in the subjective value of the food. These procedures allowed us to specify whether the OFC represents identity, sensory qualities, or the subjective value of the expected outcomes.

The primary aim of this study was to investigate the effect of nasal oxytocin on neural responses to the palatability of hedonic food. Detailed procedures and results are reported in the method section and Supplementary Information.

2. Materials and methods

2.1. Participants

Twenty-four right-handed, healthy, non-obese male participants [mean ± standard error of mean (SEM) age 27.4 ± 5.9 years, range 25–39; body mass index (BMI) 22.1 ± 2.9 kg/m^2, range 17.0–27.6] with no history of neurological or psychiatric problems were recruited from the local area via email. This study was approved by the ethical committee of the National Institute for Physiological Sciences of Japan in accordance with the Declaration of Helsinki. All participants provided written informed consent. No statistical test was performed to determine the sample size a priori. The sample size that we chose is similar to that used in previous studies (Chikazoe et al., 2014; Haxby et al., 2011; McNamee et al., 2013).

2.2. Experimental design

2.2.1. Experimental procedure

Our primary aim was to investigate the effect of nasal oxytocin on the neural responses to a change in the palatability of hedonic food. To this end, the same experimental procedure, except for drug administration (nasal oxytocin or placebo), was performed twice in two days; the two experiments were spaced 7–41 days apart (17.0 ± 9.0, mean ± standard deviation [SD]). Participants received nasal oxytocin on one experimental day and placebo on the other day, in a randomized crossover, double-blind manner. Details on the nasal oxytocin administration procedure can be found in Supplementary Methods and Supplementary Fig 1. Participants were instructed to abstain from the intake of any food and caffeinated or alcoholic beverages after 8 pm on the day preceding each experiment. The schedule on the experiment day was controlled in the same manner. Between the first and second fMRI sessions, the participants ate the standard Japanese lunch box (776 kcal). If they were not satiated, they could eat as much of the three types of snacks (chocolate cookie, salt cracker, and rice cracker) as they wished. Total calorie consumption was 802.2 ± 64.8 (mean ± SD). Moreover, the psychological and physiological hunger levels were examined. Before and after scanning, participants completed 10-cm visual analogue scales (VAS) of appetite including the question: 'How hungry do you feel right now?' Thus, participants completed the VAS rating four times on each experimental day. Before and after a meal, the experimenter used a lancet to obtain a drop of blood from the side of the finger and measured the plasma glucose level using a glucometer.

2.2.2. Visual stimuli

We collected 128 food photos from the Internet. Half of the images depicted the main dishes (mainly salty and savory), and the other half depicted desserts (mainly sweets). Detailed descriptions are provided in Supplementary Table 1. No food items in these photos were the same as those that the participants actually ate in the experiment. Every photo was resized to 600 × 400 pixels.

2.3. fMRI Task

The same fMRI experiments were conducted before and after a meal and were repeated on day 2. The only difference in the experiments performed between day 1 and 2 was drug administration (oxytocin or placebo). Thus, the participants completed four fMRI sessions. In an fMRI session, 128 food photos, 64 scrambled images, and 64 resting images (white cross in the center of a black background) were presented through four runs. The order of the 256 stimuli was fixed within an fMRI session which was composed of four runs. Each trial was fully adjacent without any ISI except for resting trials. It is recommended that trials are randomly ordered with a different randomization for each subject in the multivariate analysis (Mumford et al., 2014). However, in the current experimental setting, pseudo-randomization would cause an

undesirable effect where the same stimulus is represented differentially in each run for each subject. This effect is not preferable for the current research aim; therefore stimuli were presented in a fixed order. While participants were asked to rate the palatability of the food using a ten-point scale during the presentation of the food image, they were asked to rate the brightness of each image during the presentation of the scrambled image (1 = not at all; 10 = most ever). Each stimulus without a resting image was presented for 2900 ms, during which participants considered the rating on a 10-point scale. This was followed by the presentation of a fixation image (red cross in the center of a black background) for 1100 ms, during which participants verbally reported their rating. We chose the verbal reporting method because it allowed the participant to report scores in a fine range such as 10 points even in a very short period. Although verbal reporting might cause head movement and/or bias the ratings by "social desirability" effect (participants might feel hesitancy to report "10″ toward high calorie food), collecting more data was prioritized under the time constraint. These ratings were recorded manually by the experimenter, who was listening via an audio system connected to a microphone near the participant's mouth. During the presentation of the resting image for 4000 ms, the participants were given a break (Fig. 1A). Although a longer and jittered inter-stimulus interval (ISI) is preferred (Dale, 1999), to avoid distortion by jittering in trial-by-trial analysis, a short and fixed ISI with the resting phase as "null trial" was employed. In the post-experiment interview, it was confirmed that all food items in the fMRI sessions were familiar to the participant, given that all experimental procedures were completed each day.

2.4. Imaging parameter

MR images were collected using a 3.0 T-fMRI system (Verio; Siemens Erlangen, Germany) with a 32-element phased-array head coil. T2 * -weighted gradient echo-planar imaging (EPI) was used to obtain functional images. The sequence was as follows: repetition time (TR) = 2000 ms, echo time (TE) = 30 ms, TA = 900 ms, flip angle = 75°, field of view = 192 mm, 60 slices with isotropic 3-mm voxels, multiband EPI: multiband factor = 3. For anatomical imaging, a T1-weighted three-dimensional (3D) magnetization-prepared rapid-acquisition gradient echo (MP-RAGE) sequence was employed (TR = 1800 ms; TE = 1.98 ms; flip angle = 9°; field of view = 256 mm; and voxel dimensions = 1.0 × 1.0 × 1.0 mm).

2.5. Data analysis

2.5.1. Behavioral analysis

We conducted two-way repeated-measures analysis of variance (ANOVA) on the palatability of the food by day (days 1 and 2) and metabolic state (hungry and satiated) as factors, using SPSS 23 (See Supplementary Fig. 2). All ANOVAs and analysis of covariance (ANCOVA) in this study, including the Supplementary Results, were performed by using SPSS23. Palatability was used as a metric for the subjective value of food in this study.

2.5.2. fMRI data preprocessing for the representational similarity analysis

Standard image preprocessing was performed using the Statistical Parametric Mapping (SPM12) package in MATLAB (R2014a). As the longitudinal magnetization of the tissue already reached a steady-state before the first trial in the session because of dummy scans, we did not discard the first some volumes in each session. The functional images were realigned to correct for head motion. Each participant's T1-weighted image was co-registered with the mean image of all functional images for each participant. Accordingly, all functional images were processed by segmentation and normalization to the MNI-152 space using the unified segmentation-normalization tool in SPM12. To obtain precise voxels in the gray and white matter of each participant, the first EPI volume in the first run of day 1 was segmented into gray and white matter masks using the tissue probability map of SPM12. To construct a representational similarity matrix (RSM) that was associated with the identical objects, neural activations were estimated on a trial-by-trial basis. To estimate the brain activity evoked at each trial by regression, the response and explanatory variables were computed as follows: We extracted the BOLD signal time series for each voxel. Nuisance variables (including six head motion components encoding the x, y, and z directions and pitch, roll, and yaw for each run) and the dummy variables encoding each run, were regressed out from the data. A summary of head motion parameters is presented in Supplementary Table 2. The residual in this regression was high-pass filtered at 1/128 Hz and then used as a response variable in each voxel. To construct a design matrix for the explanatory variables, each presentation period of 128 food and 64 scrambled images was separately modeled for each

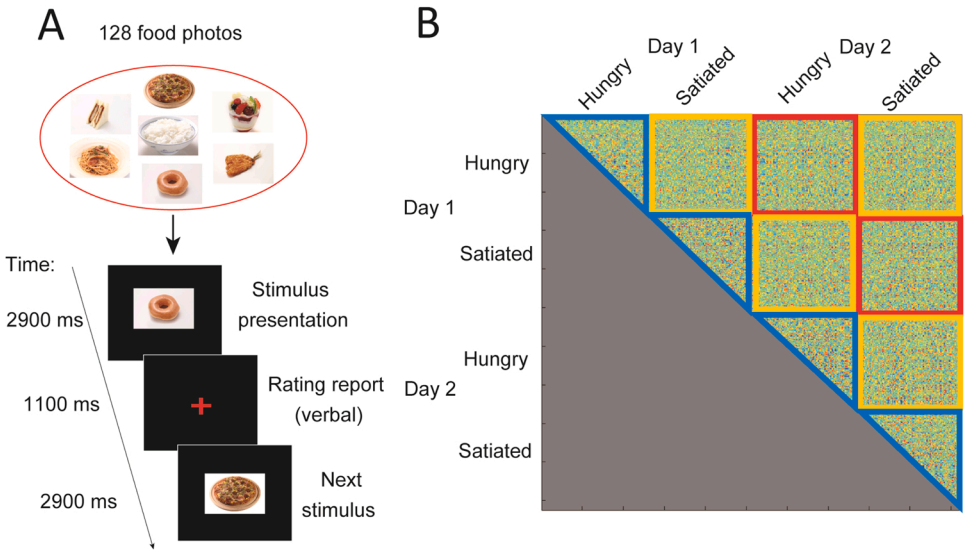

Fig. 1. Experimental task and data structure. (A) fMRI task procedure. A total of 128 food photos were presented during the fMRI sessions. Participants were instructed to determine their rating for palatability of the food using a 10-point scale during the presentation of each photo. This was followed by fixation, during which the participants reported their rating verbally. (B) Schematic illustration of the session pair structure. To conduct the representational similarity analysis, we first constructed a representational similarity matrix on a trial-by-trial basis. The 4 × 4 matrix indicates the combinations of experimental sessions (due to redundancy, only the upper triangle is shown). Each element represents an experimental session pair. Each color surrounded by a square or upper triangle represents a 128 × 128 representational similarity matrix (RSM) for each session pair. Because there were four experimental sessions in total, we analyzed 10 session pairs, including four within-session pairs (shown in blue) and six cross-session pairs (shown in red and orange). Moreover, cross-session pairs could be divided into the same metabolic state pairs (shown in red) and different metabolic state pairs (shown in orange).(For interpretation of the references to colour in this figure, the reader is referred to the web version of this article.)

stimulus, and the verbal reporting period was modeled as a regressor of no interest. The design matrix, which was high-pass filtered at 1/128 Hz and whitened, was used as the explanatory variable. By applying the ridge regression with the empirically determined ridge parameter, the brain activity evoked by each food photo stimulus was estimated on a trial-by-trial basis, resulting in 128 × 4 = 512 regression coefficients. Finally, these coefficients were transformed to t-values as estimates of the neural activity.

2.5.3. *Representational similarity analysis for identical objects and metabolic states*

Because it is difficult to directly model the effects of object specificity, metabolic states, values, and their interactions on neural responses, we employed representational similarity analysis (Kriegeskorte, 2008). All data processing of multivariate analysis in this study were performed using MATLAB (R2014a), except for the statistical tests and multiple comparisons in the group analysis of the whole brain. Our primary aim was to investigate which brain areas are associated with the representations of identical objects and whether these representations are affected by metabolic state changes. For each session pair (e.g., day 1 hungry and day 2 satiated), we estimated the neural representational similarity on a trial-by-trial basis, resulting in a 128 × 128 RSM. Because there were four experimental sessions in total, six cross-session RSMs (i.e., 4 × 3 /2 = 6) and four within-session RSMs were computed (Fig. 1B). To examine how metabolic states affected neural representations, cross-session RSMs were divided into pairs of two same and four different metabolic states (Fig. 1B). Prior to the construction of neural RSMs, 512 (128 × 4) estimates of the neural activity were de-meaned for each voxel. Using searchlight analysis (Kriegeskorte et al., 2006), correlation coefficients of activation patterns for each trial combination (128 × 128) were calculated in a spherical searchlight (radius = 5 mm), yielding the neural RSM for each session pair. Then, we calculated four representational similarity metrics, categorized as identical object pair in the same metabolic state (ISS), non-identical object pair in the same metabolic state (NSS), identical object pair in the different metabolic state (IDS) and non-identical object pair in the different metabolic state (NDS) in each gray matter voxel. The detail of these procedures is shown in Supplementary Fig. 3. To investigate the identical object specificity effect in the same and different metabolic state pairs, we calculated [ISS – NSS] and [IDS – NDS], and then the data were spatially smoothed (full width half maximum = 8 mm) for each participant. In this study, we adopted the same full-width half maximum value for smoothing in all multivariate analyses. Because we focused on representations in the cerebral cortices, we masked the information map with a cerebral cortex mask created using the SUIT anatomy toolbox (http://www.diedrichsenlab.org/imaging/propatlas.htm). Under the null hypothesis of no difference in the representational similarities between identical and non-identical object pairs, the smoothed data were subjected to a non-parametric one-sample t-test across participants, using FSL's Randomize function (v2.1, 5000 permutations). The threshold-free cluster enhancement (TFCE) correction for multiple comparisons (Smith and Nichols, 2009) was used, and the statistical threshold was set at $p < 0.05$, family wise error (FWE) (Fig. 2A). All statistical tests and multiple comparisons for group analysis of the whole brain in this study were performed using the same procedures as described above. To visualize the representations of identical objects and the effect of metabolic states on them, we conducted a region of interest (ROI) analysis. Representational similarity metrics were spatially smoothed separately for each category, as described above. We selected the primary visual area (V1) and fusiform gyrus (FG) as the ROIs in addition to the OFC. We generated three anatomically defined ROIs (V1: primary visual area, FG: fusiform gyrus, lOFC: lateral orbitofrontal cortex) based on the standard automated anatomical labeling (AAL) template (Tzourio-Mazoyer et al., 2002) within the gray matter voxels of at least 12 participants. The anatomical labels used for defining the three ROIs were as follows: V1: calcarine

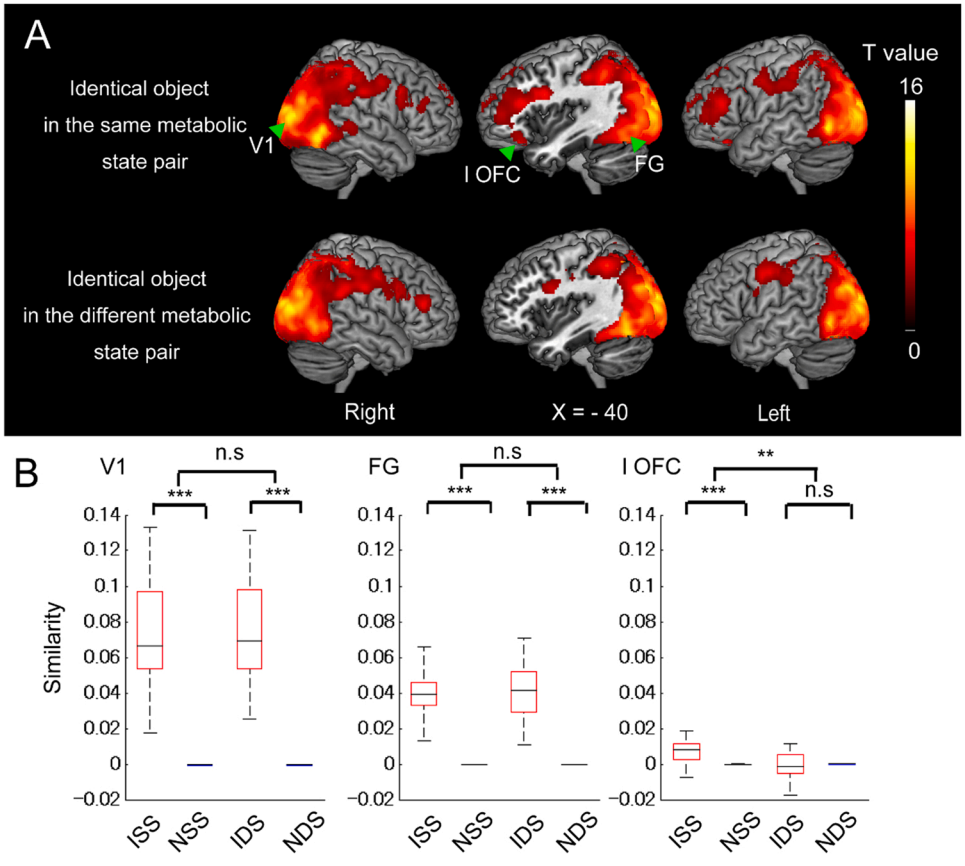

Fig. 2. Representations of identical objects in the same and different metabolic state pairs (A) The brain regions that showed higher similarity for identical objects in comparison to non-identical objects in the same (upper) and different (lower) metabolic state pairs. Color denotes t value thresholds at $p < 0.05$ (FWE). N = 24. (B) Neural representational similarity in three regions of interest: V1, primary visual area; FG, fusiform gyrus; and lOFC, lateral orbitofrontal cortex. N = 24. ISS, identical object pair in the same metabolic state; NSS, non-identical object pair in the same metabolic state; IDS, identical object pair in the different metabolic state; NDS, non-identical object pair in the different metabolic state; n.s. not significant. Boxes represent the median and 25th/75th percentiles, and whiskers represent the minimum and maximum. ***$p < 0.001$; **$p < 0.01$; Bonferroni-corrected.(For interpretation of the references to colour in this figure, the reader is referred to the web version of this article.)

gyrus; FG: fusiform gyrus; lOFC: superior orbitofrontal cortex, middle orbitofrontal cortex and inferior orbitofrontal cortex. To avoid the double dipping problem (Kriegeskorte et al., 2009), we applied a leave-one-participant-out procedure (Chikazoe et al., 2019). After excluding each of the 24 participants, we conducted non-parametric one-sample t-tests on the identical object specificity effect in the same metabolic state pair with the remaining 23 participants, resulting in 24 t-value maps. We then identified the peak voxel in the three ROIs for each map and extracted four representational similarity metrics (i.e., ISS, NSS, IDS, and NDS) in the averaged data from a spherical searchlight (radius = 5 mm) region, around the peak from the left-out participant's data (Fig. 2B). We conducted paired t-tests on the identical object specificity effect in the same and different metabolic states and the difference between these effects in the data. All t-tests on behavioral, physiological, and ROI data in this study were two-sided and Bonferroni corrected, including those in Supplementary Results.

2.5.4. Representational similarity analysis for value representations

The behavioral results indicate the possibility that the value distance distribution was correlated with the object specificity effect on neural representations in the OFC as shown in Supplementary Fig. 4 and Supplementary results. (Because the term "distance" is used to denote a dissimilarity measure in the context of representational similarity analysis (Kriegeskorte, 2008), hereafter we refer to the absolute difference of subjective values between each pair of stimuli as the value distance). To explore this possibility, we first investigated whether the OFC represented subjective values in the multivariate analyses. To use independent data from the analysis above, we used the data in the within-session pairs only (Fig. 1B, blue), which did not include data used in the analysis of identical objects. We examined how well the value distance model explained the neural representational dissimilarity. The detail of the analytic procedure to acquire the RDM relatedness metrics for each participant is shown in Supplementary Fig. 5. Under the null hypothesis of no relatedness between the value distance model RDM and neural RDM, the bias maps calculated by the permutation test were subjected to a non-parametric one-sample t-test across participants. The statistical threshold was set at $p < 0.05$ and FWE-corrected. The table reporting the clusters and their information was constructed using FSL's cluster function (Fig. 3, whole brain map; Supplementary Fig. 6, cluster list; Supplementary Table 3).

2.5.5. Value distribution adjustment

Because differences in value distance are accompanied by identity differences, to rigorously estimate the identical object specificity effect, the value distance must be controlled before being subjected to statistical tests. We developed a method in which the value distance distribution was adjusted between pairs of identical and non-identical objects. This novel method was inspired by the basic idea of age adjustment, which has been broadly used in the fields of epidemiology and public health (Curtin and Klein, 1995; Neison, 1844). Supplementary Fig. 7 shows the detail of the procedures in this method. By using these procedures, we obtained neural similarity metrics while controlling for the value effect in identical and non-identical object pairs in each session pair in each cerebral voxel. Using the procedures described above, we obtained four representational similarity metrics categorized into ISS, NSS, IDS, and NDS. To estimate the difference in identical object specificity effects between the same and different metabolic state pairs, we calculated [(ISS – NSS) – (IDS – NDS)] metrics in each gray matter voxel. After these similarity metrics were spatially smoothed for each participant, they were subjected to a one-sample t-test. The statistical threshold was set at $p < 0.05$ and FWE-corrected. The table reporting the clusters and their information was constructed using FSL's cluster function (Fig. 4A, whole brain map; Supplementary Fig 8, cluster list; Supplementary Table 4). To visualize representations of identical objects and the effect of metabolic states on them, we conducted an ROI analysis. Each representational similarity metric in the four categories described above was spatially smoothed. Using a leave-one-participant-out procedure and the lOFC ROI as in the identical object analysis, we extracted four representational similarity metrics (i.e., ISS, NSS, IDS, and NDS) (Fig. 4B). We conducted a paired t-test on identical object specificity effects in the same and different states and the difference between these effects in the data. To visualize the value representations in this searchlight region, we computed the neural representational similarities in relation to the value distance. In all within-session pair data (Fig. 1B, blue), we extracted neural RDM elements based on value distance (0, 1, 2, > 2) without value distribution adjustment in this region, and then averaged them in each bin (Fig. 4C).

2.5.6. Nasal oxytocin administration

All data in this study were derived from a project aimed at investigating the effect of nasal oxytocin on neural responses to subjective value changes. Because we did not observe any effects of oxytocin administration in behavioral analysis, physiological and neural data

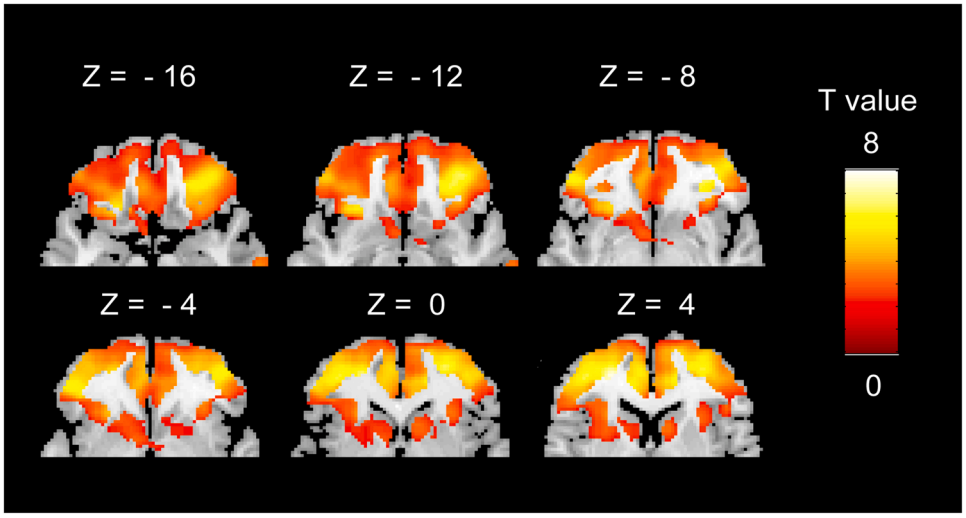

Fig. 3. Value representations in the OFC. Multivariate analysis revealed that subjective values are represented in the medial and lateral OFCs. The color denotes the t-values thresholds at $p < 0.05$, corrected (FWE). N = 24.(For interpretation of the references to colour in this figure, the reader is referred to the web version of this article.)

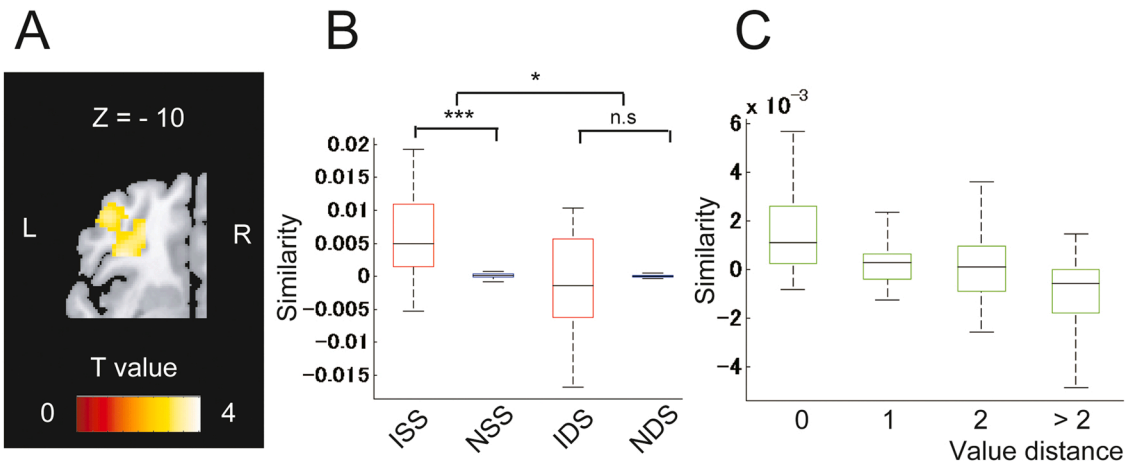

Fig. 4. Representations of sensory qualities other than the subjective value in the OFC. (A) Representational similarity analysis revealed that the left lOFC was associated with the difference of object specificity between the same and different metabolic states. Colors represent the t values thresholds at $p < 0.05$, corrected (FWE). N = 24. (B) Neural representational similarity in the lOFC. lOFC, lateral orbitofrontal cortex; ISS, identical object pair in the same metabolic state; NSS, non-identical object pair in the same metabolic state; IDS, identical object pair in different metabolic state; NDS, non-identical object pair in different metabolic state. N = 24. Boxes represent the median and 25th /75th percentiles and whiskers represent the minimum and maximum. *** $p < 0.001$; * $p < 0.05$; Bonferroni-corrected. (C) Neural representational similarity in value distance bin in the lateral OFC. N = 24. Boxes represent the median and 25th/75th percentiles and whiskers represent the minimum and maximum.(For interpretation of the references to colour in this figure, the reader is referred to the web version of this article.)

analysis, we analyzed the data assuming that the same experimental procedure was repeated on both days. The experimental procedures and results of these analyses are provided in Supplementary Methods and Results.

3. Results

3.1. Behavioral results

Twenty-four healthy male adults completed four fMRI sessions in two days before and after a meal with a total of 128 food photos presented during the fMRI sessions (Supplementary Table 1). Participants were instructed to rate the palatability of the food using a 10-point scale during the presentation of the photo in each trial (Fig. 1A). Palatability was used as a metric of the subjective value of food. The rating scores were subjected to a two-way repeated measures ANOVA with the factors of experimental day (days 1 and 2) and meal (before and after a meal) (day: $F_{1,23} = 4.06$, $p = 0.056$, partial $\eta^2 = 0.150$; meal: $F_{1,23} = 81.37$, $p = 5.15 \times 10^{-9}$, partial $\eta^2 = 0.780$; day × meal: $F_{1,23} = 2.45$, $p = 0.13$, partial $\eta^2 = 0.096$). Post-hoc simple t-tests revealed that while eating a meal significantly decreased the subjective value of the food ($t_{23} = 9.02$, $p = 1.03 \times 10^{-8}$, Cohen's $d = 1.98$), the experimental day did not have a significant effect ($t_{23} = -2.02$, $p > 0.05$, Cohen's $d = -0.14$). Although having eaten a meal decreased the palatability for all foods, the experimental day (first or second day) had no effect on palatability (Supplementary Fig. 2). Because of the numerous food stimuli, we conducted additional behavioral analysis to exclude the identical effect of the food item by using a linear mixed model with MATLAB function lme. Palatability was used as the dependent variable, the metabolic state was used as the fixed variable, and participant and food identity were used as random variables. The metabolic state change significantly decreased the palatability even when controlling participant and food identity effects ($t_{6120} = -5.61$, $p = 2.05 \times 10^{-8}$). Moreover, to evaluate the experimental duration effects on palatability, we conducted multiple regression analysis on palatability using the metabolic state, experimental day, and experimental duration as regressors. While the metabolic state change significantly decreased the palatability, the experimental day and duration did not affect it (metabolic state: standardized regression coefficient = −0.983, $t_{92} = -9.56$, $p = 1.95 \times 10^{-15}$; experimental day: standardized regression coefficient = −0.179, $t_{92} = 0.62$, $p > 0.05$; experimental interval: standardized regression coefficient = −0.233, $t_{92} = -1.23$, $p > 0.05$).

3.2. Representations of identical objects in the OFC is sensitive to metabolic state change

Our primary aim was to investigate the effect of nasal oxytocin administration; however, all analyses on the drug effect reported negative results. We, therefore, used the data to determine which brain region contributed to identical object representations and its association with the metabolic state change. To investigate the effect of metabolic state change, the representational similarity metrics of the identical and non-identical object pairs were averaged separately for pairs of the same metabolic state (two session pairs, Fig. 1B: red) and different metabolic states (four session pairs, Fig. 1B: orange) (See Supplementary Fig. 3 in detail). To estimate the object specificity effects in pairs from the same and different metabolic states, the differences in these metrics between identical and non-identical object pairs were subjected to a one-sample t-test for each voxel, separately, in two metabolic state pairs. We found that identical objects were similarly represented in the lateral OFC only in pairs of the same metabolic state, whereas identical objects were similarly represented in the V1 and FG in pairs of both the same and different metabolic states (Fig. 2A). To visualize representations of identical objects and the effect of metabolic states on them, we conducted an ROI analysis in V1, FG, and lateral OFC. Representational similarity metrics for the four categories described above are plotted in Fig. 2B. We observed the object specificity effect in the same metabolic state pair in all three regions (V1: $t_{23} = 12.11$, $p = 3.68 \times 10^{-11}$, Cohen's $d = 3.52$, FG: $t_{23} = 14.54$, $p = 8.76 \times 10^{-13}$, Cohen's $d = 4.23$, lOFC: $t_{23} = 5.10$, $p = 7.28 \times 10^{-5}$, Cohen's $d = 1.48$) and the object specificity effect in a different metabolic state pair in V1 and FG, but not in lOFC (V1: $t_{23} = 12.45$, $p = 2.10 \times 10^{-11}$, Cohen's $d = 3.62$, FG: $t_{23} = 12.88$, $p = 1.07 \times 10^{-11}$, Cohen's $d = 3.74$, lOFC: $t_{23} = -0.43$, $p > 0.05$, Cohen's $d = -0.12$). Furthermore, we found a difference in the object specificity effect across metabolic states only in the lOFC (V1: $t_{23} = -0.45$, $p > 0.05$, Cohen's $d = -0.03$, FG: $t_{23} = -0.99$, $p > 0.05$, Cohen's $d = -0.17$, lOFC: $t_{23} = 3.34$, $p = 0.0028$, Cohen's $d = 1.04$). These results demonstrated that the representations of identical objects in V1 and FG were not affected by the metabolic states, suggesting that object identity was represented in the primary and higher visual cortices. On the other hand, representations in the lOFC do not reflect pure visual features, but rather the sensory qualities of the

expected outcome, which are adaptively altered, reflecting changes in metabolic states.

3.3. State-sensitive representations of identical objects in the OFC were not explained by a change in subjective value

The results described above suggest that information about identical objects is not uniformly represented across brain regions; instead, each brain region represents different aspects of identical objects. Specifically, the representations of identical objects in the OFC are affected by metabolic state changes. Although identity refers to the physical and/or categorical aspect of a food item itself, sensory qualities refer to the uniqueness of the perceptual experience evoked by the item. This implies that a change in the metabolic state alters the inferred sensory qualities, but not the object identity. Thus, the state-sensitive representations of identical objects in the OFC, as described above, might refer to inferred sensory qualities other than object identity. However, considering the fact that previous studies have consistently demonstrated the involvement of the OFC in subjective value representation (Chikazoe et al., 2014; Gallagher et al., 1999; Gottfried et al., 2003; Kringelbach et al., 2003; Padoa-Schioppa and Assad, 2006, 2008; Stalnaker et al., 2014; Tremblay and Schultz, 1999), these results may be explained by a change in the palatability of food, accompanied by a metabolic state change (Supplementary Fig. 2). Moreover, effect of the identical object was confounded with the value distance (see Supplementary Fig. 4 and Supplementary Results). These results indicate that the difference in the value distance distribution may explain the difference in the neural representational dissimilarities between identical and non-identical object pairs. To explore this possibility, we conducted a representational similarity analysis of the value representations. To ensure data independence from the analysis of identical object representations, we used the data in only the within-session pairs (Fig. 1B; blue). After the searchlight analysis, the relatedness of the neural and value distance model RDMs was estimated based on the correlation coefficients between these RDMs (see Supplementary Fig. 5). With the permutation procedure, we computed where the actual correlation fell among the simulated null distribution of correlations, which was used for the summary statistic. In the group analysis, under the null hypothesis of no relationship between the neural and model RDMs, these summary statistics were subjected to a one-sample t-test for each voxel.

We found that subjective values were represented in multiple brain regions, including the lateral and medial OFC, precuneus, and parietal lobules (Fig. 3; for the whole brain map, see Supplementary Fig. 6; for the cluster list, see Supplementary Table 3). These results suggest that to rigorously estimate the effect of identical object specificity, the effect of value distance must be analytically dissociated from that of the metabolic change, at least in value-related regions such as the OFC. To this end, we investigated the effect of metabolic states on the representations of identical objects while controlling for the effect of value distance differences in cross-session pairs. We matched the distribution of non-identical and identical object pairs, and vice versa. Supplementary Fig. 9 provides step-by-step explanation of the analysis procedures. Supplementary Fig. 7 shows the details of this analytic procedure. Then, the representational similarity metrics in four categories (i.e. ISS, NSS, IDS and NDS) were calculated as in the identical object analysis in Fig. 2. To estimate the interaction of the object specificity and metabolic states, we calculated the difference of difference of the similarities [(ISS – NSS) – (IDS – NDS)] as the summary metric. In the group analysis, the summary metric was subjected to a one-sample t-test for each voxel.

Even after applying the distribution adjustment, we found a significant difference in identical object specificity between the same and different metabolic states in the lOFC and lateral frontal area (Fig. 4A; for the whole brain map, see Supplementary Fig. 8; for the cluster list, see Supplementary Table 4). To visualize the representations of identical objects and the effect of metabolic states on them under the value distribution control, we conducted ROI analysis in the lOFC (Fig. 4B). We adopted a leave-one-subject-out procedure (Chikazoe et al., 2019) in this analysis in the same way as in the identical object analyses in Fig. 2B (see details in Methods). This analysis revealed a significant effect of object specificity in the pairs of the same metabolic state ($t_{23} = 4.29$, $p = 5.46 \times 10^{-4}$, Cohen's $d = 1.24$) but not in pairs of different metabolic states ($t_{23} = -0.55$, $p > 0.05$, Cohen's $d = -0.16$). Furthermore, there was also a significant difference in object specificity between the same and different metabolic state pairs ($t_{23} = 2.64$, $p = 0.015$, Cohen's $d = 0.90$). To visualize the coexistence of value representations and the interaction between object specificity and metabolic states in this region, we plotted the neural representational similarity without the value distribution adjustment for each value distance bin (Fig. 4C). This revealed a monotonic decrease in representational similarity as the value distance increased, indicating that the same portion of the lOFC was associated with the interaction between object specificity and metabolic states, as well as the value.

These results demonstrate that representations of identical objects in the lOFC were altered by metabolic state changes, which was not explained by the value representations. A dendrogram in Supplementary Fig. 10 explains this logic based on the observed results. These results suggest that the lOFC integrates the visual features and infers the gustatory features, reflecting an inferred gustatory experience. We conclude that sensory qualities and subjective values of the expected outcomes coexist in the lOFC.

4. Discussion and conclusions

In this study, we explored the neural representation of object specificity and its relationship with the metabolic states, as well as the subjective values. During fMRI scanning, participants rated food palatability based on gustatory information inferred from the food photos. By applying representational similarity analysis, we revealed that object identity was represented in the primary visual cortex and FG. Although neuroimaging studies have rarely reported the involvement of the OFC in identity representations, we found that representations of identical objects were constantly maintained in the lOFC only under the same metabolic conditions. Interestingly, representations of identical objects were altered when the metabolic state changed. We also found that the OFC represents the subjective value of food objects, which is consistent with previous studies (Chikazoe et al., 2014; Gallagher et al., 1999; Gottfried et al., 2003; Kringelbach et al., 2003; Padoa-Schioppa and Assad, 2006, 2008; Stalnaker et al., 2014; Tremblay and Schultz, 1999). Importantly, the altered representation of identical objects due to a change in the metabolic state was not explained by the subjective value, which indicates the existence of integrated representations of object-specific information and metabolic states in addition to value representations in the OFC. These results suggest that the OFC does not represent pure visual features or object identity but rather represents the subjective value as well as sensory qualities of the expected outcome, which are adaptively altered, reflecting a change in the metabolic state.

4.1. Representations of identical objects in the OFC

Animal studies have consistently demonstrated that reward identity is represented by the OFC neurons. For example, rodent electrophysiological studies have indicated that OFC neurons encode specific features, which constitute the odor identity (Schoenbaum and Eichenbaum, 1995; Stalnaker et al., 2014). Similarly, single-unit recordings in monkeys revealed that OFC neurons exhibited differential responses to different odors (Cichy et al., 2011) and tastes (Padoa-Schioppa, 2007). However, the human neuroimaging literature lacks evidence for identity representations in the OFC, although several studies have revealed that the interaction of reward and identity might reside in the OFC (Howard et al., 2015; Klein-flügge et al., 2013). Identity representations are generally assumed to be associated with specific features with which an animal or human subject can discriminate one stimulus from multiple

stimuli (Cichy et al., 2011; Hung et al., 2005; Kriegeskorte et al., 2007). In this study, food objects could be identified by visual features, such as the color or shape, as well as categories. Consistent with this, representations of identical objects were similarly represented in the visual cortices, including V1 and the FG (Fig. 2). Furthermore, these representations were stable across different metabolic states, which is a requisite characteristic for "object identity' (DiCarlo et al., 2012). By contrast, representations of identical objects in the OFC were sensitive to metabolic state changes (Fig. 2). This indicates that the OFC does not represent pure visual features, but instead represents inferred sensory qualities that are adaptively altered, reflecting changes in the metabolic states. These results suggest that the OFC appears to represent reward identity, depending on the experimental setting; however, our results clearly demonstrate that the OFC does not represent mere identity, but rather represents inferred sensory qualities as well as value.

4.2. Implications for functional subdivisions in the OFC

Functional distinctions between medial and lateral OFCs have been reported in many studies (Noonan et al., 2012, 2010; Rudebeck and Murray, 2014; Wallis, 2012). Connectivity studies have revealed distinct medial and lateral orbitofrontal networks in rats (Ongür and Price, 2000), monkeys (Carmichael and Price, 1996), and humans (Kahnt et al., 2012), indicating a functional dissociation between the medial and lateral OFCs across species. Consistent with this, recent studies have demonstrated that although the lateral OFC is required for evaluating options (Rudebeck and Murray, 2011; Walton et al., 2010), the medial OFC is associated with choices among objects based on value comparisons (Boorman et al., 2009; FitzGerald et al., 2009; Hunt et al., 2012; Noonan et al., 2010; Rudebeck and Murray, 2011; Strait et al., 2014). Indeed, a recent multivariate pattern analysis of human fMRI revealed identity-specific value representations of food in the lateral OFC and identity-general value representations of food in the ventromedial prefrontal cortex (Howard et al., 2015). Moreover, another multivariate analysis of fMRI data demonstrated that although food value is represented in neural activity patterns in both the medial and lateral OFC, only the lateral OFC represents the elemental nutrient content (Suzuki et al., 2017). These results suggest that the value of objects is represented in both the medial and lateral OFCs, whereas more complicated associations that cannot be explained by value alone are represented in the lateral OFC. Consistent with this, we replicated the value representations in the medial and lateral OFCs (Fig. 3). We further demonstrated that object-specific features represented in the lateral OFC were not invariant, but rather, were flexibly altered, reflecting the internal metabolic states. These results are in line with previous connectivity studies showing sensory orbitofrontal network in the primate lateral OFC, which is characterized by connections with the gustatory, olfactory, and visual cortices (Carmichael and Price, 1996). In this network, the visual information of objects converges with the olfactory, gustatory, and visceral inputs (Rudebeck and Murray, 2011). This complex visual–chemovisceral convergence might enable the lateral OFC to play an important role in inferring specific outcomes based on integrated multidimensional information.

The limitations of the present study need to be considered. First, the sample size in the current study was relatively small and not based on a priori power analysis. A smaller sample size causes lower statistical power and consequently lower reproducibility of the results (Button et al., 2013, Ioannidis, 2018, but see Bacchetti, 2013). Second, the order of the visual stimuli was fixed within an fMRI session. It is recommended that trials are randomly ordered with a different randomization for each subject in the multivariate analysis (Mumford et al., 2014). Therefore, it is possible that both the relatively small sample size and the fixed order of the stimuli might have introduced bias to the data. However, because the pseudo-randomization might possibly cause an undesirable effect where the same stimulus is represented differentially in each run for each subject, stimuli were presented in a fixed order. Related to this issue, one might argue that the resting trials in the present study are virtually equal to jittering ISI with a duration of 0 or 4 s. Indeed, resting trials were employed to increase the estimation efficiency for the trials adjacent to the resting trials, as with jittering ISI. To compare the same item representations across experimental sessions, both the order of trials and the interval between trials including the resting trials should be fixed. As it is not clear whether jittering ISI contributes to the stability of each item representation across experimental sessions, it is worth investigating the effect of jittering ISI in future studies. Third, there was a lack of counterbalance in the order of metabolic states as the hunger state always preceded the satiated state. Although arranging four experimental sessions each other day might have solved the problem, we did not schedule them as such due to the difficulty of participant recruitment.

In summary, this study revealed that the OFC represents the inferred perceptual experience linked with the current internal state, which supports flexible decision-making. These results support the idea that representations in the OFC have unique flexible functions required for updating an individual's moment-to-moment values based on the current internal state.

Code availability

The source code of the representational similarity analyses is available at Google Drive (https://drive.google.com/drive/folders/18FYtVcEcJL2klfqbc5s1XfJQ04l7GcXj?usp=sharing).

CRediT authorship contribution statement

Takaaki Yoshimotoa: Methodology, Investigation, Writing – original draft, Writing – review & editing. **Shuntaro Okazakia:** Investigation, Writing – review & editing. **Motofumi Sumiyaa:** Investigation, Writing – review & editing. **Haruka K. Takahashic:** Investigation, Writing – review & editing. **Eri Nakagawaa:** Investigation, Writing – review & editing. **Takahiko Koikea:** Investigation, Writing – review & editing. **Ryo Kitadad:** Investigation, Writing – review & editing. **Shiki Okamotoe:** Investigation, Writing – review & editing. **Masanori Nakataf:** Writing – review & editing. **Toshihiko Yadag:** Methodology, Investigation, Writing – original draft, Writing – review & editing. **Hirotaka Kosakai:** Resources, Writing – original draft, Writing – review & editing. **Norihiro Sadato:** Writing – original draft, Writing – review & editing, Supervision. **Junichi Chikazoe:** Conceptualization, Methodology, Writing – original draft, Writing – review & editing, Supervision.

Competing interests

The Authors declare no competing interests.

Acknowledgements

This work was partly supported by JSPS KAKENHI Grant Number J15H01846 to N.S., JSPS KAKENHI Grant Number J18H05017 and J21H05060 to J.C., the Japan Agency for Medical Research and Development (AMED) under Grant Number JP19dm0207086 to J. C., and by the Japan Agency for Medical Research and Development (AMED) under Grant Number JP18dm0107152 and JP18dm0307005 to N.S. Computational resources were provided by the Data Integration and Analysis Facility, National Institute for Basic Biology, and the Research Center for Computational Science. We would like to thank Editage (www.editage.com) for English language editing.

Appendix A. Supporting information

Supplementary data associated with this article can be found in the online version at doi:10.1016/j.neures.2022.02.004.

References

Bacchetti, P., 2013. Small sample size is not the real problem. Nat. Rev. Neurosci. 14, 585. https://doi.org/10.1038/nrn3475-c3.

Boorman, E.D., Behrens, T.E.J., Woolrich, M.W., Rushworth, M.F.S., 2009. How green is the grass on the other side? Frontopolar cortex and the evidence in favor of alternative courses of action. Neuron 62 (5), 733–743. https://doi.org/10.1016/j.neuron.2009.05.014.

Burke, K.A., Franz, Theresa, M., Miller, Danielle, N., Schoenbaum, G., 2008. The role of the orbitofrontal cortex in the pursuit of happiness and more specific rewards. Nature 454 (7202), 340–344. https://doi.org/10.1038/nature06993.

Button, K.S., Ioannidis, J.P.A., Mokrysz, C., Nosek, B.A., Flint, J., Robinson, E.S.J., Munafò, M.R., 2013. Power failure: why small sample size undermines the reliability of neuroscience. Nat. Rev. Neurosci. 14 (5), 365–376. https://doi.org/10.1038/nrn3475.

Carmichael, S.T., Price, J.L., 1996. Connectional networks within the orbital and medial prefrontal cortex of macaque monkeys. J. Comp. Neurol. 371 (2), 179–207.

Chikazoe, J., Lee, D.H., Kriegeskorte, N., Anderson, A.K., 2014. Population coding of affect across stimuli, modalities and individuals. Nat. Neurosci. 17 (8), 1114–1122. https://doi.org/10.1038/nn.3749.

Chikazoe, J., Lee, D.H., Kriegeskorte, N., Anderson, A.K., 2019. Distinct representations of basic taste qualities in human gustatory cortex. Nat. Commun. 10 (1), 1–8. https://doi.org/10.1038/s41467-019-08857-z.

Cichy, R.M., Chen, Y., Haynes, J.D., 2011. Encoding the identity and location of objects in human LOC. NeuroImage 54 (3), 2297–2307. https://doi.org/10.1016/j.neuroimage.2010.09.044.

Curtin, L.R., Klein, R.J., 1995. Direct standardization (age-adjusted death rates). Healthy People 2000 Stat. Notes 6, 1–10.

Dale, A.M., 1999. Optimal experimental design for event-related fMRI. Hum. Brain Mapp. 8 (2–3), 109–114. https://doi.org/10.1002/(SICI)1097-0193(1999)8:2/3<109::AID-HBM7>3.0.CO;2-W.

DiCarlo, J.J., Zoccolan, D., Rust, N.C., 2012. How does the brain solve visual object recognition? Neuron 73 (3), 415–434. https://doi.org/10.1016/j.neuron.2012.01.010.

FitzGerald, T.H.B., Seymour, B., Dolan, R.J., 2009. The role of human orbitofrontal cortex in value comparison for incommensurable objects. J. Neurosci. 29 (26), 8388–8395. https://doi.org/10.1523/JNEUROSCI.0717-09.2009.

Gallagher, M., McMahan, R.W., Schoenbaum, G., 1999. Orbitofrontal cortex and representation of incentive value in associative learning. J. Neurosci. 19 (15), 6610–6614. https://doi.org/10.1523/JNEUROSCI.19-15-06610.1999.

Gottfried, J.A., O'Doherty, J., Dolan, R.J., 2003. Encoding predictive reward value in human amygdala and orbitofrontal cortex. Science 301 (5636), 1104–1107. https://doi.org/10.1126/science.1087919.

Gremel, C.M., Costa, R.M., 2013. Orbitofrontal and striatal circuits dynamically encode the shift between goal-directed and habitual actions. Nat. Commun. 4, 1–12. https://doi.org/10.1038/ncomms3264.

Hare, T.A., Camerer, C.F., Rangel, A., 2009. Self-control in decision-making involves modulation of the vmPFC valuation system. Science 324 (5927), 646–648. https://doi.org/10.1126/science.1168450.

Haxby, J.V., Guntupalli, J.S., Connolly, A.C., Halchenko, Y.O., Conroy, B.R., Gobbini, M.I., Hanke, M., Ramadge, P.J., 2011. A common, high-dimensional model of the representational space in human ventral temporal cortex. Neuron 72 (2), 404–416. https://doi.org/10.1016/j.neuron.2011.08.026.

Howard, J.D., Gottfried, J.A., Tobler, P.N., Kahnt, T., 2015. Identity-specific coding of future rewards in the human orbitofrontal cortex. Proc. Natl. Acad. Sci. 112 (16), 5195–5200. https://doi.org/10.1073/pnas.1503550112.

Hung, C.P., Kreiman, G., Poggio, T., Dicarlo, J.J., 2005. Fast readout of object identity from macaque inferior temporal cortex. Science 310 (5749), 863–866. https://doi.org/10.1126/science.1117593.

Hunt, L.T., Kolling, N., Soltani, A., Woolrich, M.W., Rushworth, M.F.S., Behrens, T.E.J., 2012. Mechanisms underlying cortical activity during value-guided choice. Nat. Neurosci. 15 (3), 470–476. https://doi.org/10.1038/nn.3017.

Ioannidis, J.P.A., 2018. Why most published research findings are false. Get. Good: Res. Integr. Biomed. Sci. 2 (8), 2–8. https://doi.org/10.1371/journal.pmed.0020124.

Izquierdo, A., 2004. Bilateral orbital prefrontal cortex lesions in rhesus monkeys disrupt choices guided by both reward value and reward contingency. J. Neurosci. 24 (34), 7540–7548. https://doi.org/10.1523/JNEUROSCI.1921-04.2004.

Janssen, L.K., Duif, I., van Loon, I., Wegman, J., de Vries, J.H.M., Cools, R., Aarts, E., 2017. Loss of lateral prefrontal cortex control in food-directed attention and goal-directed food choice in obesity. NeuroImage 146, 148–156. https://doi.org/10.1016/j.neuroimage.2016.11.015.

Kahnt, T., Chang, L.J., Park, S.Q., Heinzle, J., Haynes, J.-D., 2012. Connectivity-based parcellation of the human posteromedial cortex. J. Neurosci. 32 (18), 6240–6250. https://doi.org/10.1523/JNEUROSCI.0257-12.2012.

Klein-flügge, M.C., Barron, H.C., Brodersen, K.H., Dolan, R.J., Edward, T., Behrens, J., 2013. Segregated encoding of reward-identity and stimulus-reward associations in human orbitofrontal cortex. J. Neurosci. 33 (7), 3202–3211. https://doi.org/10.1523/JNEUROSCI.2532-12.2013.

Kriegeskorte, N., 2008. Representational similarity analysis - connecting the branches of systems neuroscience. Front. Syst. Neurosci. 2, 1–28. https://doi.org/10.3389/neuro.06.004.2008.

Kriegeskorte, N., Goebel, R., Bandettini, P., 2006. Information-based functional brain mapping. Proc. Natl. Acad. Sci. 103, 3863–3868. https://doi.org/10.1073/pnas.0600244103.

Kriegeskorte, N., Formisano, E., Sorger, B., Goebel, R., 2007. Individual faces elicit distinct response patterns in human anterior temporal cortex. Proc. Natl. Acad. Sci. 104 (51), 20600–20605. https://doi.org/10.1073/pnas.0705654104.

Kriegeskorte, N., Simmons, W.K., Bellgowan, P.S., Baker, C.I., 2009. Circular analysis in systems neuroscience: the dangers of double dipping. Nat. Neurosci. 12 (5), 535–540. https://doi.org/10.1038/nn.2303.

Kringelbach, M.L., 2005. The human orbitofrontal cortex: linking reward to hedonic experience. Nat. Rev. Neurosci. 6, 691–702. https://doi.org/10.1038/nrn1747.

Kringelbach, M.L., O'Doherty, J., Rolls, E.T., Andrews, C., 2003. Activation of the human orbitofrontal cortex to a liquid food stimulus is correlated with its subjective pleasantness. Cereb. Cortex. 13, 1064–1071. https://doi.org/10.1093/cercor/13.10.1064.

McNamee, D., Rangel, A., O'Doherty, J.P., 2013. Category-dependent and category-independent goal-value codes in human ventromedial prefrontal cortex. Nat. Neurosci. 16 (4), 479–485. https://doi.org/10.1038/nn.3337.

Mumford, J.A., Davis, T., Poldrack, R.A., 2014. The impact of study design on pattern estimation for single-trial multivariate pattern analysis. NeuroImage 103, 130–138. https://doi.org/10.1016/j.neuroimage.2014.09.026.

Noonan, M.P., Walton, M.E., Behrens, T.E.J., Sallet, J., Buckley, M.J., Rushworth, M.F.S., 2010. Separate value comparison and learning mechanisms in macaque medial and lateral orbitofrontal cortex. Proc. Natl. Acad. Sci. 107 (47), 20547–20552. https://doi.org/10.1073/pnas.1012246107.

Neison, F.G.P., 1844. On a method recently proposed for conducting inquiries into the comparative sanatory condition of various districts, with Illustrations, Derived from Numerous Places in Great Britain at the Period of the Last Census. J. R. Stat. Soc. The Royal Statistical Society. 7, 40–68. https://doi.org/10.2307/2337745.

Noonan, M.P., Kolling, N., Walton, M.E., Rushworth, M.F.S., 2012. Re-evaluating the role of the orbitofrontal cortex in reward and reinforcement. Eur. J. Neurosci. 35 (7), 997–1010. https://doi.org/10.1111/j.1460-9568.2012.08023.x.

Ongür, D., Price, J.L., 2000. The organization of networks within the orbital and medial prefrontal cortex of rats, monkeys and humans. Cereb. Cortex 10 (3), 206–219. https://doi.org/10.1093/cercor/10.3.206.

Padoa-Schioppa, C., 2007. Orbitofrontal cortex and the computation of economic value. Ann. N. Y. Acad. Sci. 1121, 232–253. https://doi.org/10.1196/annals.1401.011.

Padoa-Schioppa, C., Assad, J.A., 2006. Neurons in the orbitofrontal cortex encode economic value. Nature 441 (7090), 223–226. https://doi.org/10.1038/nature04676.

Padoa-Schioppa, C., Assad, J.A., 2008. The representation of economic value in the orbitofrontal cortex is invariant for changes of menu. Nat. Neurosci. 11 (1), 95–102. https://doi.org/10.1038/nn2020.

Pickens, C.L., Saddoris, M.P., Gallagher, M., Holland, P.C., 2005. Orbitofrontal lesions impair use of cue-outcome associations in a devaluation task. Behav. Neurosci. 119 (1), 317–322. https://doi.org/10.1037/0735-7044.119.1.317.

Reber, J., Feinstein, J.S., O'Doherty, J.P., Liljeholm, M., Adolphs, R., Tranel, D., 2017. Selective impairment of goal-directed decision-making following lesions to the human ventromedial prefrontal cortex. Brain 140 (6), 1743–1756. https://doi.org/10.1093/brain/awx105.

Rudebeck, P.H., Murray, E.A., 2011. Balkanizing the primate orbitofrontal cortex: distinct subregions for comparing and contrasting values. Ann. N. Y. Acad. Sci. 1239, 1–13. https://doi.org/10.1111/j.1749-6632.2011.06267.x.

Rudebeck, P.H., Murray, E.A., 2014. The orbitofrontal oracle: cortical mechanisms for the prediction and evaluation of specific behavioral outcomes. Neuron 84 (6), 1143–1156. https://doi.org/10.1016/j.neuron.2014.10.049.

Rudebeck, P.H., Saunders, R.C., Prescott, A.T., Chau, L.S., Murray, E.A., 2013. Prefrontal mechanisms of behavioral flexibility, emotion regulation and value updating. Nat. Neurosci. 16 (8), 1140–1145. https://doi.org/10.1038/nn.3440.

Schoenbaum, G., Eichenbaum, H., 1995. Information coding in the rodent prefrontal cortex. I. single-neuron activity in orbitofrontal cortex compared with that in pyriform cortex. J. Neurophysiol. 74, 733–750. https://doi.org/10.1152/jn.1995.74.2.733.

Schoenbaum, G., Roesch, M.R., Stalnaker, T.A., Takahashi, Y.K., Yuji, K., 2009. A new perspective on the role of the orbitofrontal cortex in adaptive behaviour. Nat. Rev. Neurosci. 10 (12), 885–892. https://doi.org/10.1038/nrn2753.

Schoenbaum, G., Takahashi, Y., Liu, T.L., Mcdannald, M.A., 2011. Does the orbitofrontal cortex signal value? Ann. N. Y. Acad. Sci. 1239, 87–99. https://doi.org/10.1111/j.1749-6632.2011.06210.x.

Smith, S.M., Nichols, T.E., 2009. Threshold-free cluster enhancement: addressing problems of smoothing, threshold dependence and localisation in cluster inference. NeuroImage 44, 83–98. https://doi.org/10.1016/j.neuroimage.2008.03.061.

Stalnaker, T.A., Cooch, N.K., McDannald, M.A., Liu, T.L., Wied, H., Schoenbaum, G., 2014. Orbitofrontal neurons infer the value and identity of predicted outcomes. Nat. Commun. 5, 1–13. https://doi.org/10.1038/ncomms4926.

Stalnaker, T.A., Cooch, N.K., Schoenbaum, G., 2015. What the orbitofrontal cortex does not do. Nat. Neurosci. 18 (5), 620–627. https://doi.org/10.1038/nn.3982.

Strait, C.E., Blanchard, T.C., Hayden, B.Y., 2014. Reward value comparison via mutual inhibition in ventromedial prefrontal cortex. Neuron 82, 1357–1366. https://doi.org/10.1016/j.neuron.2014.04.032.

Suzuki, S., Cross, L., O'Doherty, J.P., 2017. Elucidating the underlying components of food valuation in the human orbitofrontal cortex. Nat. Neurosci. 20, 1780–1786. https://doi.org/10.1038/s41593-017-0008-x.

Tremblay, L., Schultz, W., 1999. Relative reward preference in primate orbitofrontal cortex. Nature 398 (6729), 704–708. https://doi.org/10.1038/19525.

Tzourio-Mazoyer, N., Landeau, B., Papathanassiou, D., Crivello, F., Etard, O., Delcroix, N., Joliot, M., 2002. Automated anatomical labeling of activations in SPM using a macroscopic anatomical parcellation of the MNI MRI single-subject brain. NeuroImage 15, 273–289. https://doi.org/10.1006/nimg.2001.0978.

van der Laan, L.N., de Ridder, D.T.D., Charbonnier, L., Viergever, M.A., Smeets, P.A.M., 2014. Sweet lies: neural, visual, and behavioral measures reveal a lack of self-control conflict during food choice in weight-concerned women. Front Behav. Neurosci. 8, 1–11. https://doi.org/10.3389/fnbeh.2014.00184.

Voigt, K., Murawski, C., Speer, S., Bode, S., 2020. Effective brain connectivity at rest is associated with choice-induced preference formation. Hum. Brain Mapp. 41 (11), 3077–3088. https://doi.org/10.1002/hbm.24999.

Voigt, K., Razi, A., Harding, I.H., Andrews, Z.B., Verdejo-Garcia, A., 2021. Neural network modelling reveals changes in directional connectivity between cortical and hypothalamic regions with increased BMI. Int. J. Obes. 45 (11), 2447–2454. https://doi.org/10.1038/s41366-021-00918-y.

Wallis, J.D., 2012. Cross-species studies of orbitofrontal cortex and value-based decision-making. Nat. Neurosci. 15, 13–19. https://doi.org/10.1038/nn.2956.

Walton, M.E., Behrens, T.E.J., Buckley, M.J., Rudebeck, P.H., Rushworth, M.F.S., 2010. Separable learning systems in the macaque brain and the role of orbitofrontal cortex in contingent learning. Neuron 65 (6), 927–939. https://doi.org/10.1016/j.neuron.2010.02.027.

West, E.A., Forcelli, P.A., McCue, D.L., Malkova, L., 2013. Differential effects of serotonin-specific and excitotoxic lesions of OFC on conditioned reinforcer devaluation and extinction in rats. Behav. Brain Res. 246, 10–14. https://doi.org/10.1016/j.bbr.2013.02.027.